Ligand Control of Electronic Stability of CpCr(NO)(ligand)$_2$ Complexes

Peter Legzdins,*,† W. Stephen McNeil,† Raymond J. Batchelor,‡ and Frederick W. B. Einstein*,‡

Contribution from the Departments of Chemistry, The University of British Columbia, Vancouver, British Columbia, Canada V6T 1Z1, and Simon Fraser University, Burnaby, British Columbia, Canada V5A 1S6

Received June 15, 1995[⊗]

Abstract: Treatment of $[CpCr(NO)I]_2$ with an excess of a Lewis base, L, in CH_2Cl_2 leads to the formation of the complex salts $[CpCr(NO)(L)_2]^+[I]^-$ ($[\mathbf{1}]^+I^-$, L = NH_3; $[\mathbf{3}]^+I^-$, L = $NH_2CH_2CH{=}CH_2$; $[\mathbf{7}]^+I^-$, L = $^1/_2$en). Heating of salts $[\mathbf{1}]^+I^-$ and $[\mathbf{3}]^+I^-$ results in loss of L and formation of the neutral complexes, $CpCr(NO)(NH_2R)I$ (**2**, R = H; **4**, R = $CH_2CH{=}CH_2$), respectively. In contrast, reaction of $[CpCr(NO)I]_2$ with the bulkier NH_2CMe_3 affords the neutral $CpCr(NO)(NH_2CMe_3)I$ (**6**) directly. Sequential reaction of **6** or $CpCr(NO)(P\{OMe\}_3)I$ with $AgPF_6$ and further L affords respectively the salts $[CpCr(NO)(L)_2]^+[PF_6]^-$ ($[\mathbf{5}]^+[PF_6]^-$, L = NH_2CMe_3; $[\mathbf{8}]^+[PF_6]^-$, L = $P(OMe)_3$). All these species exhibit room-temperature ESR spectra and magnetic moments consistent with their possessing 17-valence-electron configurations. Zinc reduction of $[CpCr(NO)I]_2$ in the presence of $P(OMe)_3$ leads to the improved synthesis of the known complex $CpCr(NO)(P\{OMe\}_3)_2$ (**8**), and a similar reduction with $CNCMe_3$ affords the previously unknown $CpCr(NO)(CNCMe_3)_2$ (**9**). The solid-state molecular structures of $[\mathbf{1}]^+[BPh_4]^-\cdot$NCMe, **4**, **8**, and $[\mathbf{8}]^+[BPh_4]^-$ have been established by single-crystal X-ray crystallographic analyses which afforded the following data. $[CpCr(NO)(NH_3)_2][BPh_4]\cdot$NCMe ($[\mathbf{1}]^+[BPh_4]^-\cdot$NCMe): monoclinic, space group $P2_1/n$; $Z = 4$; $a = 9.478(3)$ Å; $b = 19.288(7)$ Å; $c = 15.427(6)$ Å; $\beta = 91.99(3)°$; $V = 2818.5$ Å^3; $T = 200$ K; $R_F = 0.038$ for 2185 data ($I_o \geq 2.5\sigma(I_o)$) and 310 variables. $CpCr(NO)(NH_2C_3H_5)(I)$ (**4**): triclinic, space group $P\bar{1}$; $Z = 2$; $a = 8.0497(8)$ Å; $b = 8.3273(17)$ Å; $c = 9.3284(9)$ Å; $\alpha = 108.182(12)°$; $\beta = 92.370(8)°$; $\gamma = 94.759(12)°$; $V = 590.54$ Å^3; $T = 295$ K; $R_F = 0.024$ for 1756 data ($I_o \geq 2.5\sigma(I_o)$) and 123 variables. $CpCr(NO)(P\{OMe\}_3)_2$ (**8**): monoclinic, space group $P2_1/a$; $Z = 8$; $a = 18.080(4)$ Å; $b = 9.320(4)$ Å; $c = 21.068(3)$ Å; $\beta = 93.02(2)°$; $V = 3545.1$ Å^3; $T = 205$ K; $R_F = 0.040$ for 3356 data ($I_o \geq 2.5\sigma(I_o)$) and 411 variables. $[CpCr(NO)(P\{OMe\}_3)_2][BPh_4]$ ($[\mathbf{8}]^+[BPh_4]^-$): monoclinic, space group $P2_1/n$; $Z = 4$; $a = 10.086(2)$ Å; $b = 22.253(3)$ Å; $c = 16.150(4)$ Å; $\beta = 90.42(2)°$; $V = 3624.7$ Å^3; $T = 195$ K; $R_F = 0.044$ for 3334 data ($I_o \geq 2.5\sigma(I_o)$) and 449 variables. Despite its 17-electron configuration, $[\mathbf{1}]^+$ does not undergo ligand substitution, nor does it effect H-atom abstraction from $HSn(n\text{-}Bu)_3$. However, it exhibits an irreversible reduction at $E_{p,c} = -1.3$ V vs SCE in THF, and zinc reduction of $[\mathbf{1}]^+$ (as its $[PF_6]^-$ salt) in the presence of CO (1 atm) affords $CpCr(NO)(CO)_2$. In a reverse manner, oxidation of **2** by $[Cp_2Fe]^+[PF_6]^-$ in acetonitrile produces $[CpCr(NO)(NCMe)_2]^+[PF_6]^-$, a salt which contains a 17-electron cation similar to $[\mathbf{1}]^+$. These experimental observations lead to the conclusion that for $CpCr(NO)L_2$ complexes, σ-base ligands stabilize the 17-electron configurations of cations whereas π-acid ligands stabilize the 18-electron configurations of the neutral congeners. Intermediate ligands (e.g. L = $P(OMe)_3$) yield complexes which are capable of existing in both forms. This trend can be rationalized by the results of an Extended Hückel analysis of the CpCr(NO) fragment and the interaction of its frontier orbitals with those of various ligands, L.

Introduction

A long-standing principle of transition-metal organometallic chemistry is the 18-valence-electron rule which states that the filling of the metal's nine available bonding (or nonbonding) valence orbitals with 18 electrons will lead to a closed-shell configuration, and, therefore, a stable complex.[1] It follows from this rule that removal of one electron, giving a 17e (17-valence-electron) compound, will yield a more reactive complex, by virtue of its possessing both electronic unsaturation and unpaired electron density. Such 17e organotransition-metal complexes have been extensively studied, and these investigations have shown that 17e species are indeed highly reactive molecules.[2−8] For instance, 17e compounds can act as potent hydrogen and halogen atom abstraction reagents,[2,3] and they are often unstable with respect to dimerization via formation of metal−metal or ligand-based carbon−carbon bonds.[3,4] Most importantly, 17e species are known to undergo ligand substitution reactions (generally via associative mechanisms) at very fast rates, often orders of magnitude faster than those of their diamagnetic, 18e analogues.[3−6] This feature allows 17e compounds to play a pivotal role in highly efficient electron-transfer catalytic cycles which take advantage of the much higher reactivity of the radical

† The University of British Columbia.

‡ Simon Fraser University.

[⊗] Abstract published in *Advance ACS Abstracts*, October 1, 1995.

(1) Collman, J. P.; Hegedus, L. S.; Norton, J. R.; Finke, R. G. *Principles and Applications of Organotransition Metal Chemistry*; University Science Books: Mill Valley, CA, 1987.

(2) Brown, T. L. In *Organometallics Radical Processes*; Trogler, W. C., Ed.; Elsevier: New York, 1990; Chapter 3.

(3) Tyler, D. R. *Prog. Inorg. Chem.* **1988**, *36*, 125.

(4) Baird, M. C. *Chem. Rev.* **1988**, *88*, 1217.

(5) Kowaleski, R. M.; Basolo, F.; Trogler, W. C.; Gedridge, R. W.; Newbound, T. D.; Ernst, R. D. *J. Am. Chem. Soc.* **1987**, *109*, 4860 and references cited therein.

(6) Trogler, W. C. In *Organometallic Radical Processes*; Trogler, W. C., Ed.; Elsevier: New York, 1990; Chapter 9.

(7) (a) Coville, N. J. In *Organometallic Radical Processes*; Trogler, W. C., Ed.; Elsevier: New York, 1990; Chapter 4. (b) Kochi, J. K. In ref 7a, Chapter 7.

(8) Kochi, J. K. *J. Organomet. Chem.* **1986**, *300*, 139.

0002-7863/95/1517-10521$09.00/0 © 1995 American Chemical Society

Table 1. Numbering Scheme, Color, Yield, and Elemental Analysis Data

complex	compd no.	color (yield, %)	elemental analysis found (calcd) C	H	N
$[CpCr(NO)(NH_3)_2]^+I^-$	$[\mathbf{1}]^+I^-$	green (94)	19.38 (19.49)	3.65 (3.60)	13.46 (13.64)
$[CpCr(NO)(NH_3)_2]^+PF_6^-$	$[\mathbf{1}]^+PF_6^-$	green (83)	18.44 (18.41)	3.30 (3.40)	12.68 (12.88)
$CpCr(NO)(NH_3)I$	**2**	green (94)	20.33 (20.64)	2.99 (2.77)	9.58 (9.63)
$[CpCr(NO)(NH_2C_3H_5)_2]^+I^-$	$[\mathbf{3}]^+I^-$	dark green (65)	33.92 (34.03)	4.89 (4.93)	10.58 (10.82)
$[CpCr(NO)(NH_2C_3H_5)_2]^+PF_6^-$	$[\mathbf{3}]^+PF_6^-$	dark green (58)	32.71 (32.52)	4.65 (4.71)	10.14 (10.34)
$CpCr(NO)(NH_2C_3H_5)I$	**4**	green (32)	29.41 (29.02)	3.82 (3.65)	8.35 (8.46)
$[CpCr(NO)(NH_2CMe_3)_2]^+PF_6^-$	$[\mathbf{5}]^+PF_6^-$	bright green (46)	36.15 (35.62)	6.21 (6.21)	9.32 (9.59)
$CpCr(NO)(NH_2CMe_3)I$	**6**	olive (84)	31.39 (31.14)	4.63 (4.65)	8.05 (8.07)
$[CpCr(NO)(en)]^+I^-$	$[\mathbf{7}]^+I^-$	pale green (92)	25.18 (25.17)	3.89 (3.92)	12.49 (12.58)
$[CpCr(NO)(en)]^+PF_6^-$	$[\mathbf{7}]^+PF_6^-$	green (84)	23.65 (23.87)	3.68 (3.72)	11.77 (11.93)
$CpCr(NO)(P\{OMe\}_3)_2$	**8**	orange (63)	33.40 (33.43)	5.82 (5.87)	3.45 (3.54)
$[CpCr(NO)(P\{OMe\}_3)_2]^+PF_6^-$	$[\mathbf{8}]^+PF_6^-$	yellow-green (54)	24.49 (24.46)	4.28 (4.29)	2.38 (2.59)
$CpCr(NO)(CNCMe_3)_2$	**9**	red (72)	57.41 (57.49)	7.24 (7.40)	13.40 (13.41)

Table 2. Selected Mass Spectral, Infrared, ESR, and Magnetic Data

complex	FAB-MS (*m/z*) (+)	(−)	IR (cm^{-1}) ν_{NO} (Nujol)	ν_{NO} (solvent)	ESR *g* value (solvent)	μ_{eff} (μ_B) (solvent)
$[\mathbf{1}]^+I^-$	181 $[P^+]$	127 $[P^-]$	1658	–	–	–
$[\mathbf{1}]^+PF_6^-$	181 $[P^+]$	145 $[P^-]$	1667	1676 (THF)	1.9863 (MeCN)	1.49 (CD_3CN)
2	291 $[P^+]$	–	1658	1669 (CH_2Cl_2)	2.0214 (CH_2Cl_2)	1.41 ($CDCl_3$)
$[\mathbf{3}]^+I^-$	261 $[P^+]$	127 $[P^-]$	1667	1672 (THF)	–	–
$[\mathbf{3}]^+PF_6^-$	261 $[P^+]$	145 $[P^-]$	1672	1683 (CH_2Cl_2)	1.9867 (CH_2Cl_2)	1.35 (CD_3CN)
4	331 $[P^+]$	–	1648	1676 (Et_2O)	2.0217 (CH_2Cl_2)	1.45 ($CDCl_3$)
$[\mathbf{5}]^+PF_6^-$	293 $[P^+]$	145 $[P^-]$	1693	1679 (CH_2Cl_2)	1.9858 (CH_2Cl_2)	
6	347 $[P^+]$	–	1651	1667 (THF)	2.0199 (CH_2Cl_2)	1.26 ($CDCl_3$)
$[\mathbf{7}]^+I^-$	207 $[P^+]$	127 $[P^-]$	1680	–	–	
$[\mathbf{7}]^+PF_6^-$	207 $[P^+]$	127 $[P^-]$	1660	1679 (MeCN)	1.9893 (MeCN)	1.20 (CD_3CN)
8	395 $[P^+]$[a]	–	1609	1623 (THF)	*c*	
$[\mathbf{8}]^+PF_6^-$	395 $[P^+]$	145 $[P^-]$	1693	1705 (THF)	2.0021 (MeCN)[d]	
9	313 $[P^+]$[b]	–	1602	1635 (THF)	*e*	

[a] EI mass spectrum, probe temperature 120 °C. [b] EI mass spectrum, probe temperature 150 °C. [c] ^1H NMR (C_6D_6) δ 4.70 (t, 5H, $^3J_{PH}$ = 2.3 Hz, Cp), 3.48 (m, 18H, Me); $^{31}P\{^1H\}$ (C_6D_6) δ 226.72. [d] A_N = 4.9 G, A_P = 48.0 G. [e] ^1H NMR (C_6D_6) δ 4.89 (s, 5H, Cp), 1.05 (s, 18H, Me).

species.[7,8] Nevertheless, it should be noted that these generalizations about 17e compounds are derived from exhaustive study of a relatively narrow range of transition-metal complexes, namely carbonyl compounds, in which the metal experiences a very strong ligand field due to the π-acidic natures of the carbonyl ligands.[9]

Our recent work with 17e species has been concerned with those complexes containing the 14e CpCr(NO) fragment and a $\{Cr(NO)\}^5$ configuration.[10] In contrast to the ligands found in most known 17e species, our systems have contained weaker-field ligands such as phosphines, halides, and alkyl groups.[11] The resulting complexes have displayed interesting, and often very surprising, properties. We now report the synthesis and characterization of a number of such compounds containing amine and phosphite ligands. As a result of these investigations, we have found that the stability of these $CpCr(NO)L_2$ compounds depends upon a combination of both the valence-electron count at the chromium center and the nature of the ligand L. When L is a π-acidic ligand, such as CO, the complex is stable as an 18e, $\{Cr(NO)\}^6$ compound but decomposes upon oxidation. Alternatively, when L is a σ-basic ligand, such as NH_3, the compound is instead stable as a 17e, $\{Cr(NO)\}^5$ cation which decomposes upon reduction. Portions of this work have been previously communicated.[12]

Results and Discussion

Synthesis of $[CpCr(NO)(L)_2]^+$ and $CpCr(NO)(L)I$ Complexes. Treatment of dimeric $[CpCr(NO)I]_2$ with an excess of either ammonia or allylamine in CH_2Cl_2 leads to the rapid formation of a complex salt of the type $[CpCr(NO)(NH_2R)_2]^+[I]^-$ in which the organometallic cation is a 17e species (eq 1). These

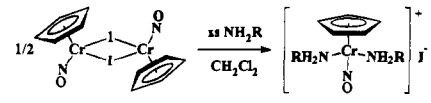

R = H, C_3H_5 (1)

salts ($[\mathbf{1}]^+I^-$, R = H; $[\mathbf{3}]^+I^-$, R = C_3H_5) result from the reaction of each half of the dimer with 2 equiv of the Lewis base, the first presumably cleaving the dimeric species and the second displacing the iodide ligand which subsequently becomes an outer-sphere anion in the salt. Both compounds are bright green, air-stable solids, which are insoluble in most common organic solvents, but soluble in polar solvents, such as THF or CH_3CN. Whereas $[\mathbf{3}]^+I^-$ is somewhat soluble in CH_2Cl_2, $[\mathbf{1}]^+I^-$ is not and precipitates immediately from the final reaction mixture. Facile metathesis of the I^- counterion in these salts for other anions such as PF_6^- renders the complexes easier to manipulate, due to a greater solubility and crystallinity of the latter salts. Consistent with the transformations summarized in eq 1, reaction

(9) Shriver, D. F.; Atkins, P.; Langford, C. H. *Inorganic Chemistry*, 2nd ed.; W. H. Freeman and Co.: New York, NY, 1994; pp 260 and 667.

(10) The Enemark–Feltham notation is a more accurate representation of electronic configuration in metal–nitrosyl complexes than is the assignment of formal oxidation states, due to the covalent nature of the M–NO linkage. The $\{Cr(NO)\}^5$ configuration can correspond approximately to a $[Cr^I(NO^+)]$ fragment if the nitrosyl is linear. Enemark, J. H.; Feltham, R. D. *Coord. Chem. Rev.* **1974**, *13*, 339.

(11) (a) Legzdins, P.; Nurse, C. R. *Inorg. Chem.* **1985**, *24*, 327. (b) Herring, F. G.; Legzdins, P.; McNeil, W. S.; Shaw, M. J.; Batchelor, R. J.; Einstein, F. W. B. *J. Am. Chem. Soc.* **1991**, *113*, 7049. (c) Legzdins, P.; McNeil, W. S.; Shaw, M. J. *Organometallics* **1994**, *13*, 562. (d) Legzdins, P.; Shaw, M. J. *J. Am. Chem. Soc.* **1994**, *116*, 7700.

(12) Legzdins, P.; McNeil, W. S.; Batchelor, R. J.; Einstein, F. W. B. *J. Am. Chem. Soc.* **1994**, *116*, 6021.

Table 3. Crystallographic Data for Complexes [**1**]$^+$[BPh$_4$]$^-$·NCMe, **4**, **8**, and [**8**]$^+$[BPh$_4$]$^-$

compound	[**1**]$^+$[BPh$_4$]$^-$·NCMe	**4**	**8**	[**8**]$^+$[BPh$_4$]$^-$
formula	$C_{31}H_{34}N_4OBCr$	$C_8H_{12}N_2OCrI$	$C_{11}H_{23}NO_7P_2Cr$	$C_{35}H_{43}NO_7BP_2Cr$
fw	541.44	331.09	395.25	714.48
cryst syst	monoclinic	triclinic	monoclinic	monoclinic
space group	$P2_1/n$	$P\bar{1}$	$P2_1/a$	$P2_1/n$
a (Å)[a]	9.478(3)	8.0497(8)	18.080(4)	10.086(2)
b (Å)	19.288(7)	8.3273(17)	9.320(4)	22.253(3)
c (Å)	15.427(6)	9.3284(9)	21.068(3)	16.150(4)
α (deg)		108.182(12)		
β (deg)	91.99(3)	92.370(8)	93.02(2)	90.42(2)
γ (deg)		94.759(12)		
V (Å^3)	2818.5	590.54	3541.1	3624.7
T (K)	200	295	205	195
Z	4	2	8	4
ρ_{calc} (g cm^{-3})	1.276	1.862	1.481	1.309
λ(Mo Kα_1) (Å)	0.70930	0.70930	0.70930	0.70930
μ(Mo Kα) (cm^{-1})	4.2	35.0	8.3	4.4
cryst dim (mm)	0.11 × 0.18 × 0.19	0.11 × 0.20 × 0.22	0.22 × 0.33 × 0.39	0.17 × 0.31 × 0.36[b] 0.28 × 0.34 × 0.40[c]
trans	0.934−0.955[d]	0.560−0.707[d]	0.715−0.802[e]	[f]
2θ range (deg)	4−45	4−50	4−45	4−45
R_F[g]	0.038	0.024	0.040	0.044
R_{wF}[h]	0.036	0.033	0.050	0.052

[a] Cell dimensions were determined from the following: 25 reflections, $24° \le 2\theta \le 34°$ ([**1**]$^+$[BPh$_4$]$^-$·NCMe); 25 reflections, $40° \le 2\theta \le 46°$ (**4**); 24 reflections, $34° \le 2\theta \le 43°$ (**8**); 25 reflections, $36° \le 2\theta \le 42°$ ([**8**]$^+$[BPh$_4$]$^-$). [b] Two crystals giving insignificantly different unit cells were used (the first was damaged by a malfunction of the LT system). For crystal #1 measured $\pm h,k,l$: $4° \le 2\theta \le 30°$ (all) and $30° \le 2\theta \le 45°$ ($0 \le k \le 2$). [c] For crystal #2 measured $\pm h,k,l$: $30° \le 2\theta \le 45°$ (all) and $4° \le 2\theta \le 15°$ ($0 \le k \le 8$). Data for the two crystals were scaled according to the intensity of a common standard reflection. For 1572 observed data pairs $R_{merge} = 0.045$. [d] The data were corrected by the Gaussian integration method for the effects of absorption. [e] The data were corrected for the anisotropic effects of absorption by the empirical method (ψ scans) and for the 2θ dependence as for a spherical crystal of radius 0.11 mm. [f] No absorption correction was applied. We estimate that this could result in a maximum possible error of F_{obs} of ±1.5%. [g] $R_F = \sum||F_o| - |F_c||/\sum|F_o|$, for 2185 ([**1**]$^+$[BPh$_4$]$^-$·NCMe), 1756 (**4**), 3356 (**8**), and 3334 ([**8**]$^+$[BPh$_4$]$^-$) data ($I_0 \ge 2.5\sigma(I_0)$). [h] $R_{wF} = [\sum(w(|F_o| - |F_c|)^2)/\sum(wF_o)^2]^{1/2}$ for observed data (see *g*, above); $w = [\sigma(F_o)^2 + kF_o^2]^{-1}$; $k = 0.0001$ ([**1**]$^+$[BPh$_4$]$^-$·NCMe), 0.0002 (**4**, and **8**), 0.0003 ([**8**]$^+$[BPh$_4$]$^-$).

of [CpCr(NO)I]$_2$ with an excess of ethylenediamine in CH_2Cl_2 leads to the immediate precipitation of analytically pure [CpCr(NO)(en)]$^+$I$^-$ ([**7**]$^+$[I]$^-$). As expected, the ethylenediamine ligand binds in a bidentate manner to the chromium center in [**7**]$^+$.[13] Again, metathesis of the I$^-$ counterion for PF_6^- is facile and leads to increased solubility. Analytical data, colors, and yields for these and all new compounds presented in this paper are found in Table 1. All these cationic species are paramagnetic, 17e complexes, as evidenced by their room-temperature ESR spectra and their magnetic moments which range from 1.2 to 1.5 μ_B (Table 2, along with mass spectral and infrared data for these and other species) and are somewhat less than the value of 1.73 μ_B expected for one unpaired electron.

The formation of complex salts in these reactions differs from previously reported reactions of [CpCr(NO)I]$_2$ with Lewis bases.[11a] In previous cases, 1 equiv of a phosphine or a phosphite was used to obtain neutral, monomeric products of the type CpCr(NO)(L)I, which are also the only products of the reaction even if an excess of the Lewis base is utilized. We have found that this is laos the case when the same reaction is performed with NH_2CMe_3. Treatment of [CpCr(NO)I]$_2$ with the sterically demanding amine leads only to CpCr(NO)(NH_2CMe_3)I (**6**) and not to the complex salt, [CpCr(NO)(NH_2CMe_3)$_2$]$^+$[I]$^-$. Consequently, the difference in the type of product obtained appears to be determined by steric rather than electronic factors, the bulkier ligands being incapable of displacing the iodide from the neutral CpCr(NO)(L)I complex. In these cases, the halide may be abstracted by a silver salt, and the second equivalent of the Lewis base is then introduced to form the desired cationic species (eq 2). This reaction sequence was known for the case where L = CH_3CN,[14] and we have found the conversions to proceed similarly for L = NH_2CMe_3 or P(OMe)$_3$ to afford the complex salts [**5**]$^+$[PF_6]$^-$ and [**8**]$^+$[PF_6]$^-$, respectively.

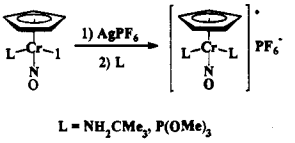

(2)

L = NH_2CMe_3, P(OMe)$_3$

It is logical that the formation of complexes [**1**]$^+$I$^-$ and [**3**]$^+$I$^-$ should proceed via the intermediate formation of the neutral CpCr(NO)(L)I compounds (**2**, L = NH_3; **4**, L = $NH_2C_3H_5$). Indeed, ESR monitoring of a CH_2Cl_2 solution of [CpCr(NO)I]$_2$ after sequential additions of $NH_2C_3H_5$ shows that the first ESR signal to appear[15] is that of **4** ($g = 2.0217$), and that as more of the amine is added, this signal is gradually replaced by that of [**3**]$^+$I$^-$ ($g = 1.9883$) (Figure 1).[16] IR monitoring of the same solutions indicates that [**3**]$^+$I$^-$ begins to form before the starting material has been entirely consumed. In other words, **4** is never the lone organometallic species in solution. Thus, reaction of [CpCr(NO)I]$_2$ with small amounts of NH_3 or $NH_2C_3H_5$ is not the method of choice for the preparation and isolation of the neutral complexes **2** or **4**. Instead, it is best to isolate the salts and then heat them in refluxing CH_2Cl_2. Under these conditions, the I$^-$ ligand re-enters the coordination sphere of the metal and the volatile amine, once displaced from the metal, is lost. In this way, both **2** and **4** may be easily obtained in analytically

(13) Similar [CpCr(NO)(L−L)]$^+$ cations have been prepared by another route. Regina, F. J.; Wojcicki, A. *Inorg. Chem.* **1980**, *19*, 3803.

(14) Chin, T. T.; Legzdins, P.; Trotter, J.; Yee, V. C. *Organometallics* **1992**, *11*, 913.

(15) [CpCr(NO)I]$_2$ exhibits no ESR signal in CH_2Cl_2 at room temperature, despite an appreciable magnetic moment in both solution and the solid state. Legzdins, P.; McNeil, W. S.; Shaw, M. J. Unpublished observations.

(16) It is interesting to note that all the neutral CpCr(NO)(L)(I) compounds exhibit a g value of approximately 2.02, while the cationic [CpCr(NO)(L)$_2$]$^+$ species have g values of about 1.99. The fortuitous separation of these signals allows for the type of monitoring depicted in Figure 1.

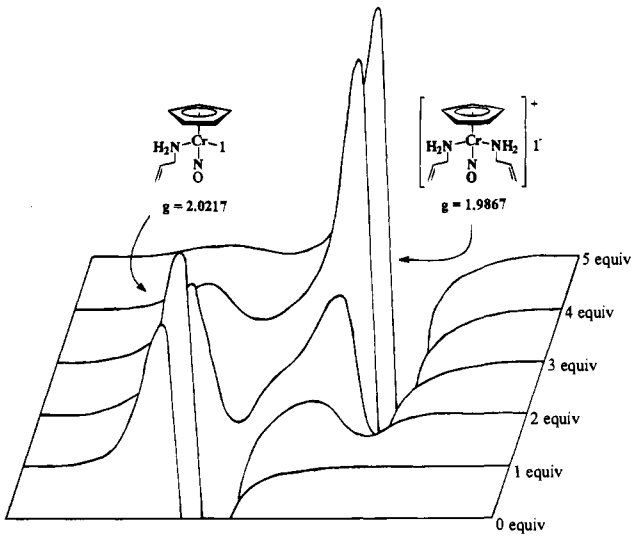

Figure 1. ESR spectra observed when $[CpCr(NO)I]_2$ in CH_2Cl_2 is treated with sequential equivalents (per chromium atom) of $NH_2C_3H_5$.

Table 4. Selected Intramolecular Distances[a] (Å) and Angles (deg) for Complexes $[1]^+[BPh_4]^-\cdot$NCMe, **4**, **8**, and $[8]^+[BPh_4]^-$

	$[1]^+[BPh_4]^-$	**4**	**8**[b]	$[8]^+[BPh_4]^-$
		Distances		
Cr–N(O)	1.665(3)	1.686(4)	1.661(4)	1.658(5)
			1.671(4)	
Cr–N(R)$_3$[c]	2.077(3)	2.085(3)		
	2.082(3)			
Cr–P			2.227(2)	2.343(2)
			−2.240(2)	2.346(3)
Cr–I		2.6739(7)		
Cr–CP[d]	1.881	1.884	1.841	1.858
			1.855	
		Angles		
Cr–N–O	170.3(3)	171.5(3)	176.9(4)	177.3(4)
			178.8(4)	
N–Cr–N(O)	97.0(1)	96.52(14)		
	98.5(1)			
P–Cr–N(O)			90.3(2)	93.4(2)
			−94.2(2)	93.8(2)
I–Cr–N(O)		97.2(1)		
$(H)_3N$–Cr–N(H)$_3$	89.6(1)			
P–Cr–P			94.77(6)	94.13(7)
			95.52(6)	
I–Cr–N(R)$_3$		91.59(8)		

[a] Thermal motion analysis (see Experimental Section) indicates that the actual bond lengths are from 0.005 to 0.010 Å longer than shown. [b] Parameters or range of parameters from two independent molecules. [c] N(R)$_3$ = NH_3 for 1^+ and $NH_2C_3H_5$ for **4**. [d] CP is the center of mass of the Cp ligand.

pure states, and they exhibit the expected room-temperature ESR spectra and magnetic moments (Table 2).

Solid-State Molecular Structures of $[1]^+$ and 4. Complexes $[1]^+$ and **4** were selected as representative examples of the cationic and neutral forms of these amine-containing 17e chromium species, respectively, and were subjected to single-crystal X-ray crystallographic analyses. X-ray quality crystals containing cation $[1]^+$ were obtained by using the bulky BPh_4^- counterion and were isolated as the acetonitrile solvate. The pertinent crystallographic and experimental data for both analyses are contained in Table 3, and selected metrical parameters are listed in Table 4. The solid-state molecular structures of $[1]^+$ and **4** are depicted in Figures 2 and 3, respectively. These structures clearly establish the monomeric natures of these compounds despite their 17e configurations and lack of steric shielding at the metal centers. Such compounds are often expected to dimerize in the absence of sterically bulky

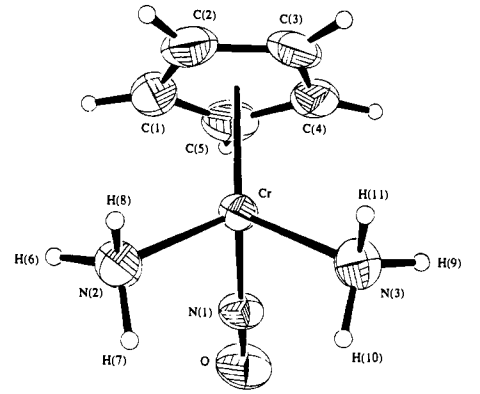

Figure 2. Structure of $[1]^+$ as it occurs in $[1]^+[BPh_4]^-\cdot$NCMe. The 50% probability displacement ellipsoids are shown for the non-hydrogen atoms and spheres or arbitrary radius for the hydrogen atoms.

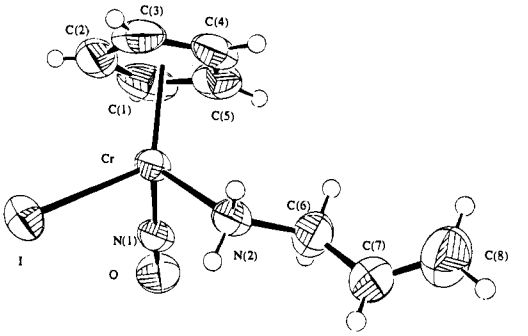

Figure 3. Structure of **4**. The 50% probability displacement ellipsoids are shown for the non–hydrogen atoms and spheres of arbitrary radius for the hydrogen atoms.

ligands via the formation of a metal–metal single bond.[4] The nitrosyl ligands in both complexes $[1]^+$ and **4** are essentially linear, as expected for a $\{M(NO)\}^5$ species,[10] and both compounds exhibit the expected three-legged piano-stool arrangement of ligands. In general, the bond lengths and bond angles in both organometallic complexes (Table 4) are normal and are comparable to those exhibited by related cyclopentadienyl chromium nitrosyl species. Thus, the amine Cr–N distances of 2.082(3) and 2.077(3) Å in $[1]^+$ and 2.085(3) Å in **4** compare well to those found in other known $\{Cr(NO)\}^5$ complexes,[17] as do the nitrosyl Cr–N distances of 1.665(3) and 1.686(4) Å.[11b,14,17,18]

Reduction and Subsequent Reactivity of $[1]^+$. When first we isolated cation $[1]^+$, we anticipated that it would be a highly reactive species, given its monomeric, 17e nature and the large and varied reactivity generally exhibited by such complexes.[2-8] In addition, the complex carries a positive charge, and its metal center is not sterically crowded (Figure 2). Both of these features might be expected to increase the reactivity of $[1]^+$ toward attack by nucleophiles. We were thus quite surprised to discover that cation $[1]^+$ is relatively inert with respect to substitution of its ligands and attack of the chromium center by nucleophiles. For example, the coordination sphere of the metal in $[1]^+$ remains intact when $[1]^+[PF_6]^-$ is dissolved in either THF or MeCN, even though both the [CpCr(NO)-

(17) Known metal–amine distances in such compounds range from 1.999(11) to 2.198(11) Å. Those greater than 2.1 Å are for amine ligands *trans* to a nitrosyl. (a) Lukehart, C. M.; Troup, J. M. *Inorg. Chim. Acta* **1977**, *22*, 81. (b) Wester, D.; Edwards, R. C.; Busch, D. H. *Inorg. Chem.* **1977**, *16*, 1055. (c) Weighart, K.; Quilitzsch, U. *Inorg. Chim. Acta* **1984**, *89*, L43. (d) Shiu, K.-B.; Chou, J. L.; Wang, Y.; Lee, G.-H. *J. Chem. Soc., Dalton Trans.* **1990**, 1989.

(18) (a) Enemark, J. H.; Quinby, M. S.; Reed, L. L.; Steuck, M. J.; Walters, K. K. *Inorg. Chem.* **1970**, *11*, 2397. (b) Ardon, M.; Cohen, S. *Inorg. Chem.* **1993**, *32*, 3241.

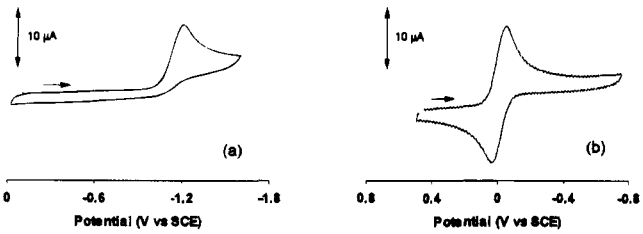

Figure 4. Ambient-temperature cyclic voltammograms of 5×10^{-4} M solutions of (a) $[\mathbf{1}]^+[PF_6]^-$ and (b) **8** in THF containing 0.1 M $[n\text{-}Bu_4N]^+[PF_6]^-$, measured at platinum-bead electrodes at scan rates of 0.4 V s^{-1}.

Table 5. Electrochemical Reduction Potentials

complex	$E_{p,c}$ (V vs SCE)[a]
$[\mathbf{1}]^+PF_6^-$	−1.24
$[\mathbf{3}]^+PF_6^-$	−1.28
$[\mathbf{8}]^+PF_6^-$	−0.03[b]

[a] Measured at a scan rate of 0.40 V/s in THF. [b] This is a reversible $E^{o\prime}$ value. Complex **8** exhibits an identical cyclic voltammogram.

$(THF)_2]^+$ [19] and $[CpCr(NO)(NCMe)_2]^+$ [14] cations are known, stable species. Furthermore, $[\mathbf{1}]^+[PF_6]^-$ in THF also does not react with either an excess of H_2O or an atmosphere of CO when stirred for 1 day at ambient temperatures. As well, $[\mathbf{1}]^+[PF_6]^-$ remains unchanged when treated with 1 equiv of $HSn(n\text{-}Bu)_3$, a common source of hydrogen atom for subsequent abstraction reactions. In all cases both the IR and ESR spectra of the reaction mixtures remain identical to those exhibited by the starting material, and $[\mathbf{1}]^+$ can be recovered unchanged as indicated by its IR and FAB-MS spectra.

Another surprising feature is the electrochemical behavior of bis(ammonia) cation $[\mathbf{1}]^+$. The cyclic voltammogram of $[\mathbf{1}]^+[PF_6]^-$ in THF (Figure 4a) reveals no oxidation features to the solvent limit and an irreversible reduction feature at −1.24 V vs SCE. Bis(allylamine) complex $[\mathbf{3}]^+PF_6^-$ exhibits a similar irreversible reduction at −1.28 V (Table 5). These unexpected observations suggest that the coordination spheres of these compounds do not remain intact upon reduction to a closed-shell, 18-valence-electron configuration which might normally be expected to be the more stable form of the complex. We reasoned that the most likely reaction the electrochemically-generated species **1** would undergo would be loss of the ammonia ligands, and we thus endeavored to effect the reduction chemically in such a way as to trap an 18e product. We succeeded in this goal by reducing $[\mathbf{1}]^+[PF_6]^-$ with an excess of Zn powder under an atmosphere of CO to obtain the known 18e $CpCr(NO)(CO)_2$ [20] complex (eq 3). In other words, whereas

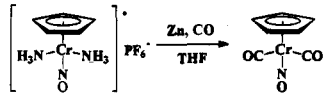

(3)

the 17-electron cation does not react with carbon monoxide under ambient conditions, its 18-electron, neutral analogue readily effects metathesis of its ammonia ligands by CO. This system is a rare example of an unreactive odd-electron organometallic species for which reduction to an even-electron configuration induces reactivity, a reversal of the commonly observed trend. Such a reversal has also been observed by Poli and co-workers for the $CpMoI_2(PMe_3)_2$ system for which an ETC ligand-substitution cycle exists with the 16e, rather than the 17e, complexes being the catalytically active species.[21]

We were also interested in determining whether the reverse process of that depicted in eq 3 could be effected, namely the oxidation of $CpCr(NO)(CO)_2$ (which exhibits an irreversible oxidation at approximately +1.2V vs SCE)[22] to form a stable 17e species. Unfortunately, attempts to effect such a conversion either chemically or electrochemically in order to form $[\mathbf{1}]^+$ are hampered by the oxidative consumption of ammonia rather than the organometallic reactant. Nevertheless, we have discovered that reaction of $CpCr(NO)(CO)_2$ with 1 equiv of $[Cp_2Fe]^+[PF_6]^-$ in acetonitrile affords the known salt[14] $[CpCr(NO)(NCMe)_2]^+[PF_6]^-$, which contains a 17e cation similar to $[\mathbf{1}]^+$ (eq 4). Without prior oxidation, $CpCr(NO)(CO)_2$ is unreactive toward acetonitrile under ambient conditions.

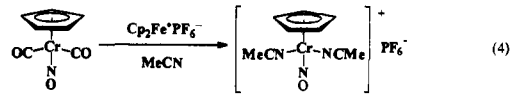

(4)

From the outcome of transformations 3 and 4 it appears that the preferred electronic configuration of $CpCr(NO)(L)_2$ molecules, i.e. the stability of the 17e paramagnetic form versus that of the 18e diamagnetic form, is determined by the nature of the ancillary ligands, L. Thus, σ-donor ligands such as NH_3 stabilize the 17e cationic compounds which decompose upon reduction to their 18e analogues. On the other hand, π-acceptor ligands such as CO evidently stabilize the 18e configuration in the neutral complexes which decompose upon oxidation to their 17e analogues. A search of the chemical literature provides further supporting evidence for this generalization. A wide range of monomeric CpCr(NO)-containing compounds are known, and those bearing σ-basic ligands are indeed 17e species[11,13,14,23] and those containing π-acidic ligands are 18e complexes.[24,25]

Given this conclusion regarding ligand control of the favored electronic configuration in these systems, it stands to reason that a ligand possessing both σ-donor and π-acceptor properties should allow for the formation of a $CpCr(NO)(L)_2$ compound between the two extremes, i.e. one stable in either the 17- or 18-valence form. $P(OMe)_3$ is just such a ligand, and we have found that the two species, $CpCr(NO)(P\{OMe\}_3)_2$ (**8**) and $[CpCr(NO)(P\{OMe\}_3)_2]^+[PF_6]^-$ ($[\mathbf{8}]^+(PF_6)^-$), may indeed be synthesized independently, the neutral form having been known to us for some time.[24a] The complexes **8** and $[\mathbf{8}]^+$ constitute the only two related compounds yet known for this system. As expected, these complexes exhibit identical cyclic voltammetry, displaying a reversible redox couple at $E^{o\prime} = -0.03$V as shown in Figure 4b. Also as expected, the IR data (Table 2) indicate

(19) $[CpCr(NO)(THF)_2]^+[PF_6]^-$ may be prepared in a manner analogous to that of $[CpCr(NO)(NCMe)_2]^+[PF_6]^-$, reaction of $[CpCr(NO)I]_2$ with $AgPF_6$ in the appropriate solvent. Legzdins, P.; Smith, K. M.; Shaw, M. J. Manuscript in preparation.

(20) Chin, T. T.; Hoyano, J. K.; Legzdins, P.; Malito, J. T. *Inorg. Synth.* **1990**, *28*, 196.

(21) Poli, R.; Owens, B. E.; Linck, R. G. *J. Am. Chem. Soc.* **1992**, *114*, 1302.

(22) Geiger, W. E.; Rieger, P. H.; Tulyathan, B.; Rausch, M. D. *J. Am. Chem. Soc.* **1984**, *106*, 7000.

(23) Fischer, E. O.; Strametz, H. *J. Organomet. Chem.* **1967**, *10*, 323.

(24) (a) Hunter, A. D.; Legzdins, P. *Organometallics* **1986**, *5*, 1001. (b) Hermann, W. A.; Hubbard, J. L.; Bernal, I.; Korp, J. D.; Haymore, B. L.; Hillhouse, G. L. *Inorg. Chem.* **1984**, *23*, 2978. (c) Behrens, H.; Landgraf, G.; Merbach, P.; Moll, M.; Trummer, K.-H. *J. Organomet. Chem.* **1983**, *253*, 217. (d) Herberhold, M.; Alt, H. *Liebigs Ann. Chem.* **1976**, 292. (e) Herberhold, M.; Alt, H.; Kreiter, C. G. *Liebigs Ann. Chem.* **1976**, 300. (f) Brunner, H. *J. Organomet. Chem.* **1969**, *16*, 119. (g) Brunner, H. *Chem. Ber.* **1969**, *102*, 305.

(25) An apparent exception is the complex $Cp^*Cr(NO)(O\text{-}i\text{-}Pr)_2$: Hubbard, J. L.; McVicar, W. K. *Inorg. Chem.* **1992**, *31*, 910. This complex is formulated as an 18e compound due to π-donation of electron density from the alkoxide groups, though the metal is in a higher formal oxidation state than in the 17e species presented here. This may well represent a third class of $Cp'Cr(NO)$ compounds, containing a formal $\{Cr(NO)\}^4$ fragment and stabilized by π-basic ligands.

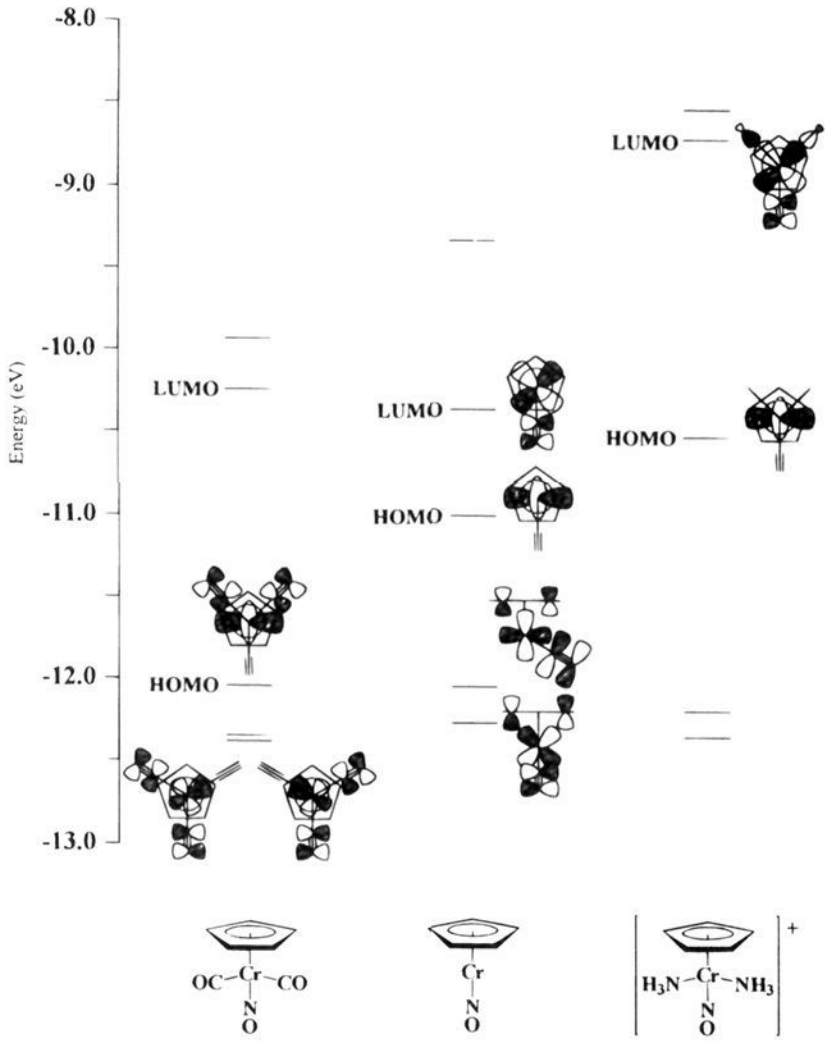

Figure 5. Molecular orbital energy diagram for the CpCr(NO) fragment, $CpCr(NO)(NH_3)_2^+$, and $CpCr(NO)(CO)_2$, indicating symmetries of selected orbitals.

Scheme 1

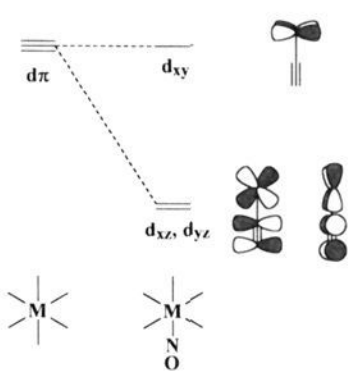

a large difference in electron density at the metal centers of **8** and $[\mathbf{8}]^+$, the nitrosyl-stretching frequencies of these compounds differing by more than 80 cm^{-1}. The spectroscopic properties of **8** have been reported previously[24a] and are given here for the sake of comparison. Those of $[\mathbf{8}]^+$ are normal, with the ESR spectrum displaying a triplet of triplets reflective of coupling to the nitrosyl ^{14}N and the two equivalent ^{31}P nuclei of the phosphite ligands (Table 2).

Metal−Ligand Bonding in the $CpCr(NO)(L)_2$ Systems. Given the unprecedented extent to which the type of ligand in this class of complexes determines the stability of a given electronic configuration, we endeavored to explain this trend on the basis of a molecular orbital description of these complexes. The results of our Extended Hückel calculations on prototypical $CpCr(NO)(L)_2$ systems are shown in Figure 5.

In the center of Figure 5 are shown the energies of the valence orbitals in the CpCr(NO) fragment as it occurs in a typical three-legged piano-stool molecule, the approximate symmetry and shape of key orbitals being as indicated. Of particular note are the natures of the three highest occupied orbitals, at −11.0, −12.1, and −12.3 eV. These three orbitals correspond approximately to those depicted in Scheme 1, which shows the perturbation of the t_{2g} set of d-orbitals in an octahedral field by the two orthogonal π^* orbitals of a nitrosyl ligand. Specifically, the HOMO in the CpCr(NO) fragment is nonbonding, and of π-symmetry, whereas the HOMO −1 and HOMO −2 orbitals represent the strongly bonding Cr−NO interaction. In the organometallic fragment these two orbitals involve a π-interaction to the Cp ligand as well. Because the HOMO is of π-symmetry, it interacts strongly with a π-acid ligand such as CO, but will not interact with a σ-base ligand such as NH_3. On the other hand, the fragment LUMO is of σ-symmetry with respect to the ancillary ligands, and will thus interact strongly with NH_3. The results of these interactions can be seen on the left and right sides of Figure 5. In $CpCr(NO)(CO)_2$ (on the left), the HOMO is primarily π-bonding to the carbonyl ligands. Thus, upon oxidation, the Cr−CO bonding orbital is reduced in electron density, the Cr−CO bonds are weakened, and the complex decomposes via loss of the CO ligands.

In the case of the 17e species (on the right side of Figure 5), the HOMO is now a singly occupied orbital (SOMO), is essentially nonbonding, and does not interact with the σ-base ligands. This feature explains the lack of coupling observed in the ESR spectra of these compounds (Table 2). In contrast, the CpCr(NO) fragment LUMO interacts strongly with the NH_3 ligands and forms a bonding and antibonding pair of molecular orbitals. The bonding orbital is very low in energy (about −14.6 eV and below the scale of Figure 5), but the antibonding orbital becomes the LUMO in the 17e complex. It is not immediately clear, therefore, why the 17e species should be unreactive toward ligand substitution. In most known cases, a reduced substitution chemistry of a 17e species is due to steric shielding of the singly occupied orbital.[4] For instance, substitution of the CO ligand in $Cp_2V(CO)$ is rapid, whereas substitution in $(\eta^5\text{-}C_5H_7)_2V(CO)$ is very slow and does not proceed associatively.[26] This is attributed to the fact that in the latter case, the SOMO is directed at the pentadienyl ligands and is sterically shielded from nucleophilic attack. Clearly, steric shielding of this nature cannot be ascribed to complex $[\mathbf{1}]^+$, since the SOMO is not directed toward the ligands, and the compound is not sterically crowded. Thus, the lack of reactivity exhibited by $[\mathbf{1}]^+$ is probably not kinetic in origin, but rather must be due to thermodynamically strong metal−NH_3 bonds. Reduction of $[\mathbf{1}]^+$ to an 18e species results in an electron-rich metal center and a weakening of the interaction with the strongly σ-basic ligands. After these ligands are lost, the complex can then be trapped by π-acidic ligands which lower the energy of the HOMO and stabilize the 18e complex. It may also be that the initial reduction product is a high-spin species resulting from the LUMO of the 17e compound becoming populated in the 18e derivative. Since the LUMO is antibonding with respect to σ-bases, this population would greatly facilitate their loss. It should be noted, however, that our calculations indicate the HOMO-LUMO gap in $[\mathbf{1}]^+$ to be greater than 1.8 eV, so it is unlikely that all of the initially reduced species will exist in its high-spin configuration.

Structural Comparison of Complexes 8 and $[\mathbf{8}]^+$. Given the molecular orbital analysis presented in the preceding section, it was of interest to us to determine what structural changes, if any, would be evident as a result of the 17e/18e redox processes in a complex which is stable in both the even- and the odd-electron configurations. Consequently, single-crystal X-ray crystallographic analyses were performed on both **8** and $[\mathbf{8}]^+[BPh_4]^-$. Despite disorder problems involving the $P(OMe)_3$ ligands, both structures refined well. The solid-state molecular structures of two adjacent and crystallographically independent molecules of **8** are shown in Figure 6, and that of $[\mathbf{8}]^+$ is

(26) Kowaleski, R. M.; Basolo, F.; Osborne, J. H.; Trogler, W. C. *Organometallics* **1988**, *7*, 1425.

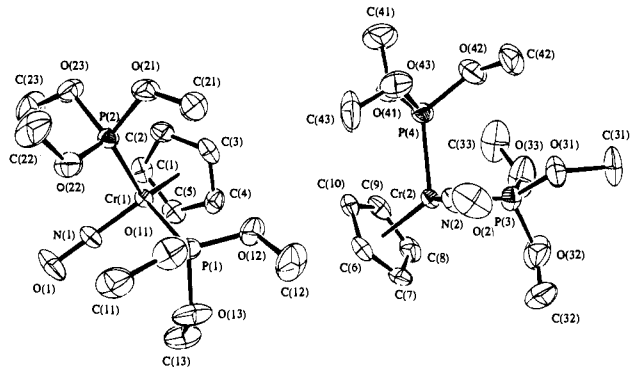

Figure 6. Structure of **8** showing two adjacent crystallographically unique molecules. The 50% probability displacement ellipsoids are shown for the non-hydrogen atoms only.

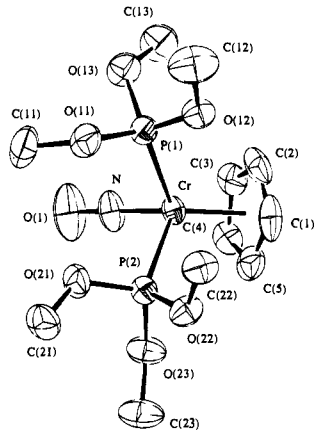

Figure 7. Structure of $[8]^+$ as it occurs in $[8]^+[BPh_4]^-$. The 50% probability displacement ellipsoids are shown for the non-hydrogen atoms. For clarity, neither the minor (9.3%) conformation for the disordered phosphite group (P(1)) nor the BPh_4^- counterion are depicted.

presented in Figure 7. The Cr−P distances of 2.3455(24) and 2.3433(14) Å in $[8]^+$ are similar to those found in other 17e chromium species such as $CpCr(NO)(PPh_3)(CH_2SiMe_3)$,[11b] $Cp^*Cr(CO)_2(PMe_3)$, and $CpCr(CO)_2(PPh_3)$.[27] The most striking difference between the structures of **8** and $[8]^+$ is that the Cr−P bond lengths are about 0.11 Å longer in the 17e cation than in the 18e neutral form. Consequently, the more electron-rich metal center binds the phosphite ligands more tightly, a feature which is exactly opposite to expectations based on simple electrostatic or ligand−field arguments. This indicates that the HOMO of the 18e complex involves a considerable π-interaction with the phosphite ligands, a conclusion in accord with the theoretical calculations presented above which indicate the HOMO to be of π-symmetry with respect to the ligands, L. Upon effecting the transformation from $[8]^+$ to **8** via reduction, this π-bonding orbital is populated to a greater extent, thereby yielding the observed stronger and shorter chromium−phosphite bonds. Conversely, oxidation from **8** to $[8]^+$ weakens these bonds, though not to the extent observed for the oxidation of $CpCr(NO)(CO)_2$ which causes the loss of the CO ligands.

Synthetic Utility of Configurational Stability in the CpCr(NO) System. The favored electronic configuration of these $CpCr(NO)(L)_2$ complexes is selectively determined to an extreme degree by the nature of the ancillary ligands, L. In addition to being highly unusual, this effect may also be exploited synthetically. The common $\{Cr(NO)\}^6$ complex in this system is $CpCr(NO)(CO)_2$, first reported over 40 years ago by Fischer.[28] The synthesis of substituted derivatives of this compound is difficult, generally requiring photolytic conditions to achieve low yields of monosubstituted complexes, CpCr(NO)(CO)L.[24c-e] A cleaner, more effective route is to synthesize derivative CpCr(NO) 18e species not by effecting substitution of an 18e starting material but rather by effecting reduction of a 17e complex in the presence of an approrpiate trapping ligand. Such a reduction renders the complex unstable, the original ligands are lost, and the $\{Cr(NO)\}^6$ fragment is stabilized by a trapping ligand appropriate to the reduced configuration, namely one that possesses some π-acid character. This synthetic method affords a simple, high-yield route to complexes such as **8** and the previously unknown $CpCr(NO)(CNCMe_3)_2$ (**9**). Effecting complete substitution of CO ligands in metal carbonyl complexes to obtain derivative species is often difficult; the technique of reducing a higher-valent complex to a lower oxidation state in order to obtain such compounds has been employed previously by us[24a,29] and others.[30]

In future studies with these $CpCr(NO)(L)_2$ complexes we shall endeavor to ascertain whether the synthetic methods outlined in this paper may be utilized for the preparation of complexes in which the ligands, L, are unsaturated organic molecules such as olefins, dienes, or acetylenes and whether these latter ligands also exert a profound influence on the preferred electronic configurations of their complexes.

Experimental Section

All reactions and subsequent manipulations were performed under anaerobic and anhydrous conditions using an atmosphere of dinitrogen. General procedures routinely employed in our laboratories have been described previously.[31] The complexes $[CpCr(NO)I]_2$,[11a] $CpCr(NO)(CO)_2$,[20] $[CpCr(NO)(NCMe)_2]^+[PF_6]^-$,[14] $CpCr(NO)(P\{OMe\}_3)I$,[11c] and $[Cp_2Fe]^+[PF_6]^-$ [32] were prepared by published procedures. Allylamine and *tert*-butylamine (Aldrich) were subjected to two freeze−pump−thaw degas cycles and were vacuum transferred from CaH_2. All other reagents were purchased from commercial suppliers and used as received. Filtrations were performed through Celite (1 × 2 cm) supported on a medium porosity glass frit unless otherwise specified. Fast-atom bombardment (6 kV ion source, 7−8 kV xenon FAB gun) mass spectra were recorded on a AEI MS9 spectrometer using 3-nitrobenzyl alcohol as a matrix. ESR spectra were recorded on an ECS 106 spectrometer at room temperature. Evans'-method magnetic measurements were effected by measuring the difference in chemical shift between the residual solvent peaks of a C_6D_6, $CDCl_3$, or CD_3CN solution of the analyte and of the pure solvent in a sealed capillary within the NMR tube. Susceptibilities were corrected for diamagnetic ligand contributions.[33]

Color, isolated yields, and analytical data for all products are listed in Table 1. Mass, IR, and ESR spectral data, along with magnetic-moment data, are collected in Table 2. Electrochemical reduction potentials are listed in Table 5.

Electrochemical Measurements. General methodology employed during cyclic voltammetry studies in our laboratories has been described

(27) Fortier, S.; Baird, M. C.; Preston, K. F.; Morton, J. R.; Ziegler, T.; Jaeger, T. J.; Watkins, W. C.; MacNeil, J. H.; Watson, K. A.; Hensel, K.; Le Page, Y.; Charland, J.-P.; Williams, A. J. *J. Am. Chem. Soc.* **1991**, *113*, 542.

(28) Fischer, E. O.; Beckert, O.; Hafner, W.; Stahl, H. O. *Z. Naturforsch., B* **1955**, *10*, 598.

(29) (a) Debad, J. D.; Legzdins, P.; Young, M. A. *J. Am. Chem. Soc.* **1993**, *115*, 2051. (b) Christensen, N. J.; Hunter, A. D.; Legzdins, P. *Organometallics* **1989**, *8*, 930.

(30) See, for example: Hessen, B.; Meetsma, A.; van Bolhuis, F.; Teuben, J. H. *Organometallics* **1990**, *9*, 1925.

(31) Dryden, N. H.; Legzdins, P.; Rettig, S. J.; Veltheer, J. E. *Organometallics* **1992**, *11*, 2583.

(32) Jolly, W. L. *The Synthesis and Characterization of Inorganic Compounds*; Prentice-Hall: Englewood Cliffs, NJ, 1970; p 487.

(33) (a) Sur, S. K. *J. Magn. Reson.* **1989**, *82*, 169. (b) Carlin, R. L. *Magnetochemistry*; Springler-Verlag: New York, 1986.

previously.[34] The three-electrode cell consisted of a Pt-bead working electrode (~1 mm diameter), a coiled Pt-wire auxiliary electrode, and a Ag/AgCl pseudoreference electrode. THF was twice distilled, first from CaH_2 and then from sodium benzophenone, and vacuum transferred from sodium benzophenone just prior to use. The electrochemical cell was assembled and used in a glovebox. Voltages are reported versus the saturated calomel electrode (SCE) and were measured using an internal ferrocene standard, the highly reversible Cp_2Fe/Cp_2Fe^+ couple occurring at +0.55 V vs SCE in THF under these conditions.

Molecular Orbital Calculations. Extended Hückel theory calculations[35] were carried out with the aid of HyperChem for Windows Release 3 and ChemPlus extensions for HyperChem, both being commercially available software packages. In all cases, single-point calculations were performed on the structures obtained from single-crystal X-ray crystallographic analyses using an unweighted Hückel constant of 1.75.

Preparation of $[CpCr(NO)(NH_3)_2]^+I^-$ ($[1]^+I^-$). $[CpCr(NO)I]_2$ (274 mg, 0.500 mmol) was placed in a Schlenk tube and was dissolved in CH_2Cl_2 (20 mL). An excess of ammonia was added in the form of ~3 mL of an ammonia-saturated CH_2Cl_2 solution. The brown reaction mixture rapidly deposited a bright green precipitate which was collected on a frit, washed with CH_2Cl_2 (2 × 10 mL), and dried in vacuo to obtain analytically pure $[1]^+I^-$.

Preparation of $[CpCr(NO)(NH_3)_2]^+[PF_6]^-$ ($[1]^+[PF_6]^-$). Solid $[1]^+I^-$ (0.308 g, 1.00 mmol) and $AgPF_6$ (0.253 g, 1.00 mmol) were placed into a Schlenk tube. The solids were stirred in MeCN (10 mL), whereupon a yellow-white precipitate was deposited. The mixture was filtered, and the green filtrate was taken to dryness in vacuo. The remaining residue was triturated and washed with pentane (2 × 10 mL), and the resulting green solid was recrystallized from CH_2Cl_2/hexanes to obtain analytically pure $[1]^+[PF_6]^-$ as green blocks.

The analogous tetraphenylborate salt, $[1]^+[BPh_4]^-$, was prepared and isolated in a similar manner using $NaBPh_4$, and X-ray quality crystals of this complex were obtained as the acetonitrile solvate (i.e. $[1]^+[BPh_4]^-\cdot NCMe$) by slow diffusion of pentane into a saturated acetonitrile solution.

Preparation of $CpCr(NO)(NH_3)I$ (2). A sample of $[1]^+I^-$ (154 mg, 0.500 mmol) was suspended in CH_2Cl_2 (100 mL), and the mixture was refluxed for 18 h. The resulting green solution was concentrated under reduced pressure. Hexanes were added, and the solution was further concentrated and cooled at −30 °C overnight in order to induce the deposition of green, crystalline **2**.

Preparation of $[CpCr(NO)(NH_2C_3H_5)_2]^+I^-$ ($[3]^+I^-$). THF (~10 mL) and an excess of allylamine were vacuum transferred onto $[CpCr(NO)I]_2$ (0.274 g, 0.500 mmol) in a Schlenk tube. The solution was warmed to room temperature and stirred for 10 min, during which time the color changed from brown to bright green. The solvent was removed in vacuo, the green residue was triturated and washed with pentane (2 × 15 mL), and the green solid was recrystallized from CH_2Cl_2/hexanes to obtain green needles of $[3]^+I^-$.

Preparation of $[CrCr(NO)(NH_2C_3H_5)_2]^+[PF_6]^-$ ($[3]^+[PF_6]^-$). Solid $[3]^+I^-$ (128 mg, 0.33 mmol) and $AgPF_6$ (84 mg, 0.33 mmol) were weighed into a Schlenk tube and stirred in CH_2Cl_2 (15 mL). A yellow-white precipitate formed immediately, and the mixture was filtered. The green filtrate was concentrated and cooled at −30 °C overnight to induce the deposition of green crystals of $[3]^+[PF_6]^-$.

Preparation of $CpCr(NO)(NH_2C_3H_5)I$ (4). A sample of $[3]^+I^-$ (388 mg, 1.00 mmol) was dissolved in CH_2Cl_2 (20 mL), and the solution was refluxed overnight. The solvent was removed in vacuo from the final mixture, and the green residue was triturated and extracted with Et_2O (2 × 15 mL). The extracts were filtered, leaving behind a green insoluble material (presumably unreacted $[3]^+I^-$). The yellow-green filtrate was concentrated, hexanes were added, and the solution was cooled at −30 °C overnight to induce the deposition of X-ray quality prisms of **4**.

Preparation of $CpCr(NO)(NH_2CMe_3)I$ (6). THF (~10 mL) and an excess of *tert*-butylamine were vacuum transferred onto $[CpCr(NO)I]_2$ (0.274 g, 0.500 mmol) in a Schlenk tube. The solution was warmed to room temperature and stirred for 10 min, during which time the color changed from brown to bright green. The solvent was removed in vacuo, the olive green residue was triturated and washed with pentane (2 × 15 mL), and the green solid was recrystallized from CH_2Cl_2/hexanes to obtain green prisms of **6**.

Preparation of $[CpCr(NO)(NH_2CMe_3)_2]^+[PF_6]^-$ ($[5]^+[PF_6]^-$). THF (~10 mL) was vacuum transferred onto a mixture of solid **6** (219 mg, 0.500 mmol) and $AgPF_6$ (183 mg, 0.500 mmol). The mixture was warmed to room temperature and stirred for 5 min, whereupon a yellow precipitate formed. The mixture was then filtered, and the frit was washed with a minimum of CH_2Cl_2. An excess of *tert*-butylamine was vacuum transferred into the filtrate, and the mixture was stirred for 2 h. The solvent was removed in vacuo, and the green residue was recrystallized from CH_2Cl_2 to obtain forest green prisms of $[5]^+[PF_6]^-$.

Preparation of $[CpCr(NO)(en)]^+I^-$ ($[7]^+[I]^-$). $[CpCr(NO)I]_2$ (274 mg, 0.500 mmol) was dissolved in CH_2Cl_2 (20 mL), and ethylenediamine (80 μL, 0.72 mg, 1.2 mmol) was added to the solution. The brown reaction mixture rapidly deposited a flocculent pale green precipitate which was collected on a frit, washed with CH_2Cl_2 (2 × 10 mL), and dried in vacuo to obtain analytically pure $[7]^+I^-$.

Preparation of $[CpCr(NO)(en)]^+[PF_6]^-$ ($[7]^+[PF_6]^-$). Solid $[7]^+I^-$ (305 mg, 0.913 mmol) and $AgPF_6$ (240 mg, 0.913 mmol) were dissolved and stirred in MeCN (10 mL), resulting in the immediate formation of a yellow precipitate. The mixture was filtered, and the solvent was removed from the filtrate in vacuo. The resulting green solid was washed and triturated with CH_2Cl_2 (15 mL) and dried in vacuo to obtain analytically pure $[7]^+[PF_6]^-$.

Preparation of $CpCr(NO)(P\{OMe\}_3)_2$ (8). The following is a modification of the previously published procedure for the synthesis of this complex.[24a] THF (~10 mL) was vacuum transferred onto $[CpCr(NO)I]_2$ (274 mg, 0.500 mmol) and Zn (0.35 g, excess, 5.4 mmol). $P(OMe)_3$ (0.25 mL, 0.26 g, 2.1 mmol) was added. The mixture was stirred at room temperature for 3 h, after which time the color of the solution had changed from green to orange. The solvent was then removed in vacuo. The solid residue was extracted with Et_2O (2 × 30 mL), and the extracts were filtered through a column (1 × 2 cm) of alumina I supported on a medium porosity glass frit. The filtrate was reduced in volume to 10 mL, and pentane (10 mL) was added. The solution was left to stand at −30 °C overnight, whereupon orange blocks of analytically pure **8** were deposited.

Preparation of $[CpCr(NO)(P\{OMe\}_3)_2]^+[PF_6]^-$ ($[8]^+[PF_6]^-$). THF (~10 mL) was vacuum transferred onto $CpCr(NO)(P\{OMe\}_3)I$ (100 mg, 0.25 mmol) and $AgPF_6$ (63 mg, 0.25 mmol), and the mixture was warmed to room temperature and stirred for 5 min, whereupon a flocculent precipitate formed. The reaction mixture was filtered, and $P(OMe)_3$ (29 μL, 31 mg, 0.25 mmol) was added to the filtrate via syringe. The mixture was then stirred overnight, the solvent was removed in vacuo, and the green residue was washed with Et_2O (2 × 10 mL). The first wash had a pale lime green color, but the second was colorless. The remaining ether-insoluble, yellow-green powder was dried in vacuo to obtain analytically pure $[8]^+[PF_6]^-$.

Preparation of $CpCr(NO)(CNCMe_3)_2$ (9). THF (~10 mL) was vacuum transferred onto solid $[CpCr(NO)I]_2$ (137 mg, 0.250 mmol) and Zn powder (0.16 g, excess) in a vessel equipped with a Telflon Rotoflow stopcock. To the solution was added *tert*-butyl isocyanide (250 μL, 184 mg, 2.21 mmol), and the reaction mixture was stirred for 3 h, after which time the solution had changed from brown to red-orange. The solvent was removed in vacuo, and the residue was extracted with 1:1 pentane/Et_2O (2 × 15 mL) and filtered through Florisil (2 × 3 cm) on a medium porosity glass frit. The filtrate was concentrated slowly in vacuo to obtain **9** as red blocks.

Dissolution of $[1]^+[PF_6]^-$ in THF or MeCN. A sample of $[CpCr(NO)(NH_3)_2]^+[PF_6]^-$ (65 mg, 0.20 mmol) was dissolved in either THF or MeCN (5 mL) in a Schlenk tube. In both cases, the green solution was stirred at ambient temperatures for 24 h, during which time no change was observed in either the IR or ESR spectra of either solution. The starting material was recovered from the final solution and was identified as unchanged by its characteristic IR, ESR, and mass spectra.

Exposure of $[1]^+[PF_6]^-$ to H_2O. A sample of $[CpCr(NO)(NH_3)_2]^+[PF_6]^-$ (65 mg, 0.25 mmol) was dissolved in THF (5 mL) in a Schlenk tube. Deaerated H_2O (1.0 mL, excess) was added to the

(34) Herring, F. G.; Legzdins, P.; Richter-Addo, G. B. *Organometallics* **1989**, *8*, 1485.

(35) Ammeter, J. H.; Bürgi, H.-B.; Thibeault, J. C.; Hoffmann, R. *J. Am. Chem. Soc.* **1978**, *100*, 3686.

solution via syringe. The reaction mixture was stirred at ambient temperatures for 24 h, during which time no change occurred in either the IR or ESR spectra of the solution.

Exposure of [1]$^+$[PF$_6$]$^-$ to CO. A sample of [CpCr(NO)(NH$_3$)$_2$]$^+$[PF$_6$]$^-$ (250 mg, 0.75 mmol) was dissolved in THF (10 mL) in a vessel equipped with a Telflon Rotoflow stopcock. The solution was placed under an atmosphere of CO and was stirred for 1 week. After this time, the IR spectrum of the final green solution revealed only one nitrosyl band, namely that due to the starting material. When a second sample was stirred in the presence of Zn powder (98 mg) under identical experimental conditions, the IR spectrum of the final solution revealed nitrosyl and carbonyl bands attributable to both [1]$^+$[PF$_6$]$^-$ and CpCr(NO)(CO)$_2$. Chromatography of the solution on a column of silica gel (3 × 10 cm) made up in pentane with pentane as the eluent resulted in the development and collection of an orange band. The eluate was taken to dryness in vacuo to obtain bright orange CpCr(NO)(CO)$_2$ (54 mg, 36% yield) which was identified by its characteristic IR and mass spectra.

Exposure of [1]$^+$[PF$_6$]$^-$ to HSn(*n*-Bu)$_3$. A sample of [CpCr(NO)(NH$_3$)$_2$]$^+$[PF$_6$]$^-$ (50 mg, 0.15 mmol) was dissolved in THF (10 mL) in a vessel equipped with a Telflon Rotoflow stopcock. HSn(*n*-Bu)$_3$ (60 μL, 82 mg, 0.23 mmol, 1.6 equiv) was added via syringe. The reaction mixture was stirred at room temperature for 24 h, during which time no change was observed in either the IR or ESR spectra of the solution. The starting material was recovered from the final solution and was identified as unchanged by its IR, ESR, and mass spectra.

Reaction of CpCr(NO)(CO)$_2$ with [Cp$_2$Fe]$^+$[PF$_6$]$^-$. CpCr(NO)(CO)$_2$ (0.100 g, 0.491 mmol) and [Cp$_2$Fe]$^+$[PF$_6$]$^-$ (0.161 g, 0.488 mmol) were weighed into a Schlenk tube and dissolved in MeCN (30 mL). The reaction mixture was stirred for 4 days at ambient temperatures. The solvent was then removed in vacuo, and the green residue was washed with Et$_2$O (3 × 30 mL). The resulting green solid (0.11 g, 60% yield) was identified as [CpCr(NO)(NCMe)$_2$]$^+$[PF$_6$]$^-$ by comparison of its ESR, IR, and mass spectral properties with those displayed by an authentic sample.

X-ray Structure Determination of Complexes [1]$^+$[BPh$_4$]$^-$·NCMe, 4, 8, and [8]$^+$[BPh$_4$]$^-$. All crystals were sealed in glass capillaries under a dry oxygen-free dinitrogen atmosphere using a trace of Apiezon grease as an adhesive. Data were recorded with an Enraf Nonius CAD4F diffractometer using graphite monochromatized Mo Kα radiation and an in-house modified low-temperature attachment. Two standard reflections per hour were measured in each case and exhibited small intensity variations (~±2%). For **8** a step-drop in intensity of ~10% occurred after an interruption in the low-temperature control. A similar event in the case of [8]$^+$[BPh$_4$]$^-$ made it necessary to use a second crystal to complete the measurements. The second crystal yielded cell dimensions which were indistinguishable from those of the first. Data for [1]$^+$[BPh$_4$]$^-$·NCMe and **4** were corrected for absorption by the Gaussian integration method.[36] The data for **8** were corrected for the anisotropic effects of absorption empirically[37] (ψ scans) and for the 2θ dependence as for a spherical crystal of radius 0.11 mm. In the case of [8]$^+$[BPh$_4$]$^-$, no absorption correction was applied, and we thus estimate that the maximum possible error in a value of F_{rel} would be ±1.5%. Data for the two crystals of [8]$^+$[BPh$_4$]$^-$ were scaled according to the intensity of a common standard reflection—for 1572 redundant data pairs R_{merge} = 0.045. Data reduction included corrections for intensity-scale variations and for Lorentz and polarization effects. The structures were solved and elaborated using standard methods.

In the case of [1]$^+$[BPh$_4$]$^-$·NCMe, nearly all the hydrogen atoms could be clearly located in an electron-density difference map but were, nonetheless, placed in calculated positions with isotropic temperature factors initially proportionate to the equivalent isotropic temperature factors of the atoms to which they were bound. For the NH$_3$ and CH$_3$ groups the calculated hydrogen atom positions were idealized, based upon the positions of the appropriate electron-density difference peaks. In subsequent cycles of refinement the coordinate shifts for the hydrogen atoms of the phenyl and cyclopentadienyl groups were linked with those for their respectively bound carbon atoms. Both NH$_3$ and CH$_3$ were refined as rigid groups subject to restraints which maintained approximate axial symmetry with respect to their N−Cr or C−C bonds. A mean isotropic temperature factor was refined for each of the following groups of hydrogen atoms and the shifts applied to the individual values: all phenyl hydrogen atoms; the cyclopentadienyl hydrogen atoms; the methyl hydrogen atoms; the hydrogen atoms of each NH$_3$ group, separately. When anisotropic thermal parameters were introduced for all non-hydrogen atoms, each phenyl group was then refined as a rigid group to reduce the number of parameters. While these constraints were maintained in the final refinement (the results of which are reported here), further refinement including independent coordinates and anisotropic thermal parameters for all non-hydrogen atoms converged in two cycles and produced neither significant shifts in any parameter nor improvement in the agreement. The final full-matrix least-squares refinement of 310 parameters (including an extinction parameter of 0.59(12) μm)[38] for 2185 observations and 9 restraints converged (maximum |shift/e.s.d.| = 0.01) at R = 0.038. The maximum peak in the final difference map (0.25(6) e Å^{-3}) occurred 1.30 Å from Cr and 0.88 Å from N(3).

For **4**, coordinates and anisotropic displacement parameters for all non-hydrogen atoms were refined. The hydrogen atom parameters were again initially assigned. In subsequent cycles of refinement the coordinate shifts for the hydrogen atoms were linked with those for the atoms to which they were bound. A single parameter was refined for the isotropic displacement for each of four groups of hydrogen atoms—those of Cp, NH$_2$, methylene and vinyl groups—and the shifts applied to the individual values. The final full-matrix least-squares refinement of 123 parameters (including an extinction parameter of 0.032(18) μm)[38] for 1756 observations converged (maximum |shift/e.s.d.| = 0.01) at R = 0.024. The maximum peak in the final difference map (0.64(8) e Å^{-3}) occurred 0.85 Å from I.

For the structures of **8** and [8]$^+$[BPh$_4$]$^-$, coordinates and anisotropic displacement parameters for all non-hydrogen atoms were again refined. Hydrogen atoms were treated as above—i.e. calculated and riding, during refinement, on their associated carbon atoms with a single isotropic displacement parameter for the hydrogen atoms of each Cp, Ph, or Me group. Electron-density difference map features indicated possible partial disorder in some of the P(OMe)$_3$ groups. This is a frequently encountered feature for this type of ligand and is often not modeled well.

In the most noticeable case here (P(1)/P(101) in [8]$^+$[BPh$_4$]$^-$), a 0.907(5)/0.093 two-site model for the disorder was developed, with the aid of appropriate restraints and contraints, in which the ligand is rotated about the Cr−P bond vector and slightly displaced to one side accompanied by changes in the Cr−P−O−C torsion angles. The major (90.7%) sites were allowed independent coordinates and anisotropic displacement parameters. The PO$_3$ fragment of the minor (9.3%) orientation was given as assigned arrangement based on that of the original ordered model and was then refined as a rigid group. The two conformations appear to coincide at C(12) and therefore this atom was treated as ordered (anisotropic). The other carbon atom sites were allowed independent coordinates. The pair C(13) and C(113) were only slightly spaced and were constrained to share a common set of anisotropic displacement parameters. The anisotropic displacement parameters for P(1) and P(101) were similarly constrained. Restraints to the O(113)−C(113) bond length, the P(101)−O(113)−C(113) bond angle, and for null-motion along the O(113)−C(13) bond were retained in the final refinement. The remaining 9.3%-occupied non-hydrogen sites were assigned initial reasonable isotropic displacement parameters, and a common parameter was refined for their isotropic displacements. Hydrogen atom parameters, including appropriate occupancy, were calculated, included, and constrained as in the preceding structures. Eleven isotropic displacement parameters were refined for the hydrogen atoms of the Cp group: each of six methyl groups (or disordered pair); each of the four phenyl groups. The single relative occupancy parameter for all the disordered atom sites was refined such that the total occupancy for this P(OMe)$_3$ group remained 1. The final full-matrix least-squares refinement for [8]$^+$[BPh$_4$]$^-$ of 449 parameters for

(36) Busing, W. R.; Levy, H. A. *Acta. Crystallogr.* **1957**, *10*, 180.
(37) North, A. C. T.; Phillips, D. C.; Mathews, F. S. *Acta. Crystallogr., Sect. A* **1968**, *24*, 351.
(38) Larson, A. C. In *Crystallographic Computing*; Ahmed, F. R., Ed.; Munksgaard: Copenhagen, 1970; p 293.
(39) Gabe, E. J.; LePage, Y.; Charland, J.-P.; Lee, F. L.; White, P. S. *J. Appl. Crystallogr.* **1989**, *22*, 384.

3334 observations and 3 restraints converged (maximum |shift/e.s.d.| = 0.04) at $R = 0.044$. The most significant positive feature in the final difference map was 0.33(6) e Å^{-3} at 1.14 Å from P(101), 1.17 Å from P(1), and 1.70 Å from Cr.

While the above model accounted reasonably well for the disorder of one $P(OMe)_3$ group the electron density difference features associated with the other one in $[\mathbf{8}]^+[BPh_4]^-$ and the four in **8** (two independent molecules) were more subtle and not simply interpretable. These groups were therefore treated as ordered with anisotropic displacement parameters for the non-hydrogen atoms. For **8**, the final full-matrix least-squares refinement of 411 parameters for 3356 observations converged (maximum |shift/e.s.d.| = 0.02) at $R = 0.040$). The largest peak in the final difference map was 0.71(7) e Å^{-3} at 1.30 Å from O(42), 1.39 Å from O(43), 1.48 Å from C(42) and 1.62 Å from P(4).

The programs used for absorption corrections, data reduction, structure solution, and graphical output were from the NRCVAX Crystal Structure System.[39] Refinement was carried out using CRYSTALS.[40] Complex scattering factors for neutral atoms[41] were used in the calculation of structure factors. Weighting schemes, based on counting statistics, for which $\langle w|F_o| - |F_c|)^2\rangle$ was nearly constant as a function of both $|F_o|$ and sin (θ/λ), were used. Computations were carried out on MicroVAX-II and 80486 computers. Crystallographic data for all four structures are collected in Table 3.

For each structure, anisotropic displacement parameters of the complexes were analyzed according to rigid body,[42] segmented rigid body model,[43] and riding[44] models for thermal motion. For $[\mathbf{1}]^+$, analysis in terms of a segmented rigid body model, in which the Cp group was allowed internal libration about the axis passing through the chromium atom and the center of mass of the cyclopentadienyl group, gave $R_w = 0.053$ for the agreement between observed and calculated U_{ij} with a root-mean-square deviation for the weighted ΔU_{ij} of 0.0011 Å^2. For **4**, a similar segmented rigid body thermal motion analysis of the anisotropic atomic-displacement parameters of the molecule—again using a model in which the Cp group is allowed internal libration about the Cr-to-Cp (center of mass) axis—yielded $R_w = 0.034$ for the agreement between observed and calculated U_{ij} with a root-mean-square deviation for the weighted ΔU_{ij} of 0.0010 Å^2. In the cases of **8** and $[\mathbf{8}]^+$, analogous analyses were based upon only the anisotropic displacement parameters of each $CpCrNP_2$ fragment. For the two independent molecules of **8**, values of $R_w = 0.056$, 0.054 and root-mean-square deviations of 0.0009 and 0.0010 Å^2, respectively, were obtained. For $[\mathbf{8}]^+$, $R_w = 0.068$ and the root-mean-square deviation was 0.0016 Å^2. Corrected bond lengths based upon these models and riding models for the N—O bond lengths and the C(7)—C(8) bond length in **4** are included as supporting information. Selected metrical parameters for $[\mathbf{1}]^+$, **4**, **8**, and $[\mathbf{8}]^+$ are included in Table 5.

Acknowledgment. We are grateful to the Natural Sciences and Engineering Research Council of Canada for support of this work in the form of grants to P.L. and F.W.B.E. and a postgraduate scholarship to W.S.M.

Supporting Information Available: Tables of fractional coordinates and displacement parameters, selected intramolecular distances and angles, supplementary crystallographic data for structural determinations, hydrogen atom coordinates, anisotropic thermal parameters, torsion angles, and least-squares planes for complexes $[\mathbf{1}]^+[BPh_4]^-\cdot NCMe$, **4**, **8**, and $[\mathbf{8}]^+[BPh_4]^-$ (44 pages). This material is contained in many libraries on microfiche, immediately follows this article in the microfilm version of the Journal, can be ordered from ACS, and can be downloaded from the Internet; see any current masthead page for ordering information and Internet access instructions.

JA9519546

(40) Watkin, D. J.; Carruthers, J. R.; Betteridge, P. W. *CRYSTALS*; Chemical Crystallography Laboratory, University of Oxford: Oxford, England, 1984.

(41) *International Tables for X-ray Crystallography*; Kynoch Press: Birmingham, England, 1975; Vol. IV, p 99.

(42) Shoemaker, V.; Trueblood, K. N. *Acta. Crystallogr., Sect. B* **1968**, *24*, 63.

(43) Trueblood, K. N. *Acta. Crystallogr., Sect. A* **1978**, *34*, 950.

(44) Busing, W. R.; Levy, H. A. *Acta. Crystallogr.* **1964**, *17*, 142.